This article was published in

Kanervo, J.M., Keskitalo, T.J., Slioor, R.I., Krause, A.O.I., Temperature-programmed desorption as a tool to extract quantitative kinetic or energetic information for porous catalysts, Journal of Catalysis 238 (2006) 382-393.

Available online at www.sciencedirect.com
SCIENCE DIRECT
Journal of Catalysis 238 (2006) 382–393
JOURNAL OF CATALYSIS
www.elsevier.com/locate/jcat

Temperature-programmed desorption as a tool to extract quantitative kinetic or energetic information for porous catalysts

J.M. Kanervo *, T.J. Keskitalo, R.I. Slioor, A.O.I. Krause

Laboratory of Industrial Chemistry, Helsinki University of Technology, P.O. Box 6100, FI-02015 TKK, Finland

Received 22 August 2005; revised 15 December 2005; accepted 22 December 2005

Available online 27 January 2006

Abstract

Temperature-programmed desorption (TPD) from high-surface area heterogeneous catalysts was investigated as a transient kinetic tool for studying reaction kinetics of elementary gas–solid interactions. TPD experiments carried out in flow setups have only rarely been used for kinetic purposes. Kinetic analysis of this kind of system requires a description of the extrinsic dynamics of the TPD system (i.e., the reactor flow model and intraparticle mass transfer). These were the focus of this study. In addition, the significance of the readsorption of the adsorbate was assessed. A range of process conditions and experimental parameters typical for a flow TPD setup was defined. Simulations were carried out for a single catalyst particle in TPD assuming infinite external mass transfer. The selection of the flow model for the TPD reactor was considered. Finally, the system was studied with a complete heterogeneous model for TPD consisting of a plug flow reactor model and taking into account intraparticle diffusion and intrinsic adsorption/desorption in the predefined range of parameters. The simulation results were then compared with results of previous studies on the methodology of TPD. It is concluded that the extrinsic dynamics of TPD can be coherently modelled to allow kinetic analysis according to general principles of transient kinetics, and a reappraisal of TPD as a kinetic tool for the study of high-surface area catalysts is in order. TPD may help bridge material and pressure gaps between catalysis studies and surface science studies. TPD experiments combined with kinetic analysis may also serve as a useful tool for studying microkinetics of heterogeneous catalysis.

Keywords: Heterogeneous catalysts; Temperature-programmed desorption; Kinetic analysis

1. Introduction

Temperature-programmed desorption (TPD), or flash desorption, was first described as a quantitative analytical tool for surface characterisation of low-surface area samples in ultra-high vacuum (UHV) [1]. The potential of this method to extract adsorption energies was also demonstrated. TPD was later proposed for the study of high-surface area catalysts under carrier gas and ambient pressure [2]. Today a vacuum setup is customarily used for surface science studies, and both flow and vacuum setups are widely used for catalysis studies [3].

Kinetic information on desorption is routinely extracted from UHV TPD [3]. Phenomenological interpretation of atmospheric TPD data of porous samples in terms of kinetic models is relatively uncommon and has been discouraged by some scientists [4]. Criticism has been levelled at the validity of both the extrinsic and intrinsic mathematical descriptions of the system. Table 1 describes the features of the two TPD systems. The conditions and consequent interpretation of TPD experiments can be selected from the standpoint of either surface science or engineering; solid materials can be investigated

Table 1
Features of the two TPD set-ups

UHV TPD, low surface area samples
+ allows direct assessment of intrinsic desorption kinetics
− ideal materials: material gap
− UHV: pressure gap
Atmospheric TPD, porous samples
− multiple rate processes overlap: indirect assessment of kinetics
+ practical heterogeneous catalyst materials
+ conditions are close to real operating conditions of catalytic processes

* Corresponding author.
E-mail addresses: jaana.kanervo@hut.fi, jaana.kanervo@tkk.fi (J.M. Kanervo).

0021-9517/$ – see front matter
doi:10.1016/j.jcat.2005.12.026

as ideal materials under ideal conditions or as actual catalytic materials under conditions much closer to the operating conditions in a chemical reactor. This dual nature of TPD potentially provides a means to bridge the material and pressure gaps in heterogeneous catalysis.

The kinetic interpretation of data obtained in UHV differs from that obtained at ambient pressure. UHV TPD data for single crystals allows direct assessment of the intrinsic desorption kinetics, whereas TPD from an atmospheric flow setup experiment for porous samples requires consideration as well of the mass transfer issues, such as intraparticle diffusion and the reactor flow model. The complex nature of TPD of high-surface area catalysts due to multiple overlapping rate processes necessitates a proper description of the extrinsic dynamics before analysis for intrinsic kinetics may be pursued. In addition, with TPD of porous samples it is probably not possible to study one-directional desorption because readsorption occurs.

Many methodological aspects associated with the description of the TPD system were dealt with in papers published in the late 1970s and the 1980s [5–19]. The methodology of atmospheric TPD has received less attention afterward. Although an adequate description of the physicochemical system is case-specific, most characteristics of the generally applied setups and process conditions fall within a relatively limited range. Therefore, it would be worthwhile to set up general guidelines for an appropriate description of the extrinsic dynamics for TPD within a defined range of experimental parameters. This would allow later concentration on the real interest: kinetic modelling of the rates of intrinsic gas–solid interactions. The present computational resources allow simulations based on a detailed physicochemical description of TPD systems and nonlinear regression-based model testing and parameter estimation. Nonetheless, the models used in kinetic analysis should describe the underlying phenomena that actually contribute to the observed rates of desorption.

In the present study, we investigated the prerequisites for valid transient kinetic analysis of TPD data. We reviewed and investigated the description of the extrinsic dynamics of TPD for porous samples under continuous flow at ambient pressure. This is accomplished with representative numerical simulations, theoretical considerations, and some experimental data. This study concentrates on a typical range of TPD parameters. We examine separately the behaviour of a single catalyst particle with infinite external mass transfer as an informative limiting case (Section 3.1—Part I) and the selection of the reactor flow model (Section 3.2—Part II). Finally, using the findings of Sections 3.1 and 3.2—Parts I and II, simulations with a full heterogeneous reactor model for TPD (Section 3.3—Part III) are carried out, and the significance of the results for kinetic analysis of experimental TPD data is discussed.

2. Parameters and computational details

2.1. Parameters of TPD experiment

The simulations were performed with a range of conditions and properties typical for an atmospheric TPD experiment. The parameters were selected on the basis of the literature and our experience with TPD experiments and are listed in Table 2. A single value was chosen for parameters of lesser interest. The solid sample was assumed to be a porous catalyst of small particle size, and the TPD setup was considered to be a flow reactor of packed-bed type operating under atmospheric pressure. The reactor geometry for simulations was chosen with the bed length exceeding the diameter.

Table 2
Properties and parameters of typical TPD carried out in flow set-up

Carrier gas	He/Ar
Adsorbate	$H_2/O_2/N_2/NH_3/CO/CO_2$
Flow rate of carrier gas, Q (cm^3/min)	20–120
Catalyst weight, m_{cat} (mg)	30–1900 (typically <300 mg)
Particle size radius, R_p (cm)	0.004–0.02
Catalyst density, ρ_p (mg/cm^3)	1000
Reactor	Quartz u-tube fixed bed
Bed length, L (cm)	0.4–4
Diameter, d_b (cm)	0.4–1.0 (in simulations 0.4)
Heating rate, β (K/min)	5–25 (in simulations 25)
Temperature range (K)	50–1500
Particle porosity, ε_p	0.4
Bed porosity, ε_b	0.4
Effective diffusivity in particle, D_e (cm^2/s)	0.01–0.3
Number of active sites, N_A ($\mu mol/mg_{cat}$)	0.2–1.2 (in simulations 0.5)
Pre-exponential factor of desorption, A_d (1/s)	10^{13}–10^{16}
Activation energy of desorption, E_d (kJ/mol)	50–200
Pre-exponential factor of adsorption, A_a ($cm^3/(\mu mol\,s)$)	10^4–10^7
Activation energy of adsorption, E_a (kJ/mol)	0–10 (in simulations 0)

The intrinsic kinetics was chosen to be of first order for adsorption and desorption with Langmuir assumptions,

$$\frac{d\theta_A}{dt} = k_a c_A(1-\theta_A) - k_d\theta_A. \quad (1)$$

The magnitudes of the pre-exponentials of the rate constants k_a and k_d were selected in accordance with transition state theory [20], and a reasonably broad range of activation energies of desorption was chosen. Adsorption was treated in simulations as nonactivated. The pre-exponential factors for adsorption corresponding to transition state theory [20] were transformed into the concentration units applied in this study, rounded to the precision of one significant digit.

The effective diffusion coefficient in a particle was selected to range from the order of magnitude of molecular diffusion for dilute binary gas mixtures to the order of magnitude of Knudsen diffusion. For typical values of particle porosity, constriction factor, and tortuousity, the effective diffusion coefficient should range from one-fifth to a few hundredths of the molecular diffusion [21]. The maximum heating rate ($dT/dt = \beta = 25$ K/min) was applied to induce maximum transience.

2.2. Computational details

Simulations were carried out with transient pseudohomogeneous PFR, CSTR, and convection-axial dispersion models;

a transient single-particle model with infinite external mass transfer; and the heterogeneous PFR model with intraparticle dynamics connected. (By pseudohomogeneous reactor model, we mean a situation in which intraparticle diffusion is so rapid so as to not influence the system dynamics.) The models relevant to the simulations are shown later (Table 4; Eqs. (4), (5), (15), and (16)).

The differential equations were solved in Mathworks Inc. MATLAB® 6.5 using the sparse system ODE solver ode15s. The absolute and relative ODE-solver tolerances for all variables were 10^{-8} and 10^{-10}, respectively. Partial differential equations were solved by discretising them with respect to position coordinates with equidistant spacing and treating time as a continuous variable. Diffusion-related derivatives were approximated by three-point central differences, and convection-related derivatives were approximated by three-point backward differences. A sufficient number of lattice points was selected for each case to provide stable solutions. The computer codes were validated by, for example, checking the conservation of mass in TPD by calculating the total amount desorbed from the reactor,

$$n_{\mathrm{A,sim}} = \int_{t_0}^{t_\mathrm{f}} c_{\mathrm{A,out}}(t) \cdot Q(t)\,\mathrm{d}t, \tag{2}$$

and by comparing this with the initial amount adsorbed ($n_{\mathrm{A,initial}} = \theta_{\mathrm{A,initial}} \cdot N_\mathrm{A} \cdot m_\mathrm{cat}$). In single-particle simulations, the flux out of the particle was integrated over time and compared with the initial amount adsorbed in a particle.

To quantify the difference between any two TPD curves, necessary in the comparison of model solutions, we used a root mean square error (RMSE) between them as a measure,

$$\mathrm{RMSE} = \sqrt{\frac{1}{N}\sum_{i=1}^{N}\big(\mathrm{curve}_1(i) - \mathrm{curve}_2(i)\big)^2}. \tag{3}$$

However, RMSE is dependent on the scale of the thermograms. To compare results of experiments of different scales, we also calculated a scaled RMSE (SRMSE), defined as RMSE divided by the maximum value of the two TPD responses. For an SRMSE $\leqslant 0.0450$, the two thermograms were considered equal, which corresponds to a minor deviation, comparable to typical experimental uncertainty.

3. Simulation results

3.1. Part I: Intraparticle dynamics in TPD

The behaviour of a single catalyst particle with infinite external mass transfer was studied by simulations. Although this behaviour has no exact counterpart in TPD experiments, it is approached in a vacuum TPD setup with a high pumping speed (UHV), or at the very entrance of a flow TPD reactor where the particles encounter the pure carrier gas.

Table 3
Values of the rate parameters in the simulations for a single particle

k_a ($\mathrm{cm^3/(\mu mol\,s)}$)	k_d (1/s)	$D_\mathrm{e}/R_\mathrm{p}^2$ (1/s)
$k_\mathrm{a}(\mathrm{zero}) = 0$	$k_\mathrm{d}(\mathrm{min}) = 10^{13}\exp(-200kJ/(RT))$	$D_\mathrm{e}/R_\mathrm{p}^2\ (\mathrm{min}) = 25$
$k_\mathrm{a}(\mathrm{min}) = 10^4$	$k_\mathrm{d}(\mathrm{med}) = 10^{13}\exp(-125kJ/(RT))$	$D_\mathrm{e}/R_\mathrm{p}^2\ (\mathrm{max}) = 18750$
$k_\mathrm{a}(\mathrm{max}) = 10^7$	$k_\mathrm{d}(\mathrm{max}) = 10^{16}\exp(-50kJ/(RT))$	

Mass transfer by effective diffusion and intrinsic kinetics described with Eq. (1) are assumed for the particle,

$$\frac{\mathrm{d}c_\mathrm{A}}{\mathrm{d}t} = \frac{D_\mathrm{e}}{R_\mathrm{p}^2\varepsilon_\mathrm{p}}\left(\frac{\mathrm{d}^2c_\mathrm{A}}{\mathrm{d}z^2} + \frac{2}{z}\frac{\mathrm{d}c_\mathrm{A}}{\mathrm{d}z}\right) + \frac{\rho_\mathrm{p}N_\mathrm{A}}{\varepsilon_\mathrm{p}}\left(-\frac{\mathrm{d}\theta_\mathrm{A}}{\mathrm{d}t}\right). \tag{4}$$

The first boundary condition (Eq. (5a)) is due to symmetry reasons at the particle core ($z = 0$), and the second boundary condition (Eq. (5b)) represents the infinite external mass transfer (at $z = 1$),

$$\left.\frac{\mathrm{d}c_\mathrm{A}}{\mathrm{d}z}\right|_{z=0} = 0 \tag{5a}$$

and

$$c_\mathrm{A}|_{z=1} = 0. \tag{5b}$$

Zero concentration at the outer boundary of the particle is an informative limiting case, because concentration gradients and coverage gradients in the particle cannot possibly be more drastic in a realistic TPD reactor.

For a single particle, we define the "TPD response" as the flux through the outer surface of the particle,

$$W = D_\mathrm{e}4\pi R_\mathrm{p}\left.\frac{\mathrm{d}c_\mathrm{A}}{\mathrm{d}z}\right|_{z=1}. \tag{6}$$

Different combinations of the rates of adsorption, desorption, and pore diffusion are tested to assess the interplay between the intrinsic kinetics and mass transfer. Key interests are possible diffusion limitations and the extent of readsorption in TPD. The extreme values of k_a, k_d, and $D_\mathrm{e}/R_\mathrm{p}^2$ ratio (reported in Table 2) are applied in the simulations. In addition to the extreme values, the tested values include $k_\mathrm{a}(\mathrm{zero}) = 0$ for negligible adsorption and $k_\mathrm{d}(\mathrm{med})$ for a medium desorption rate, summarised in Table 3.

The temperature range of possible TPD responses generated by the model with the tested parameter values is wide. The TPD responses for the extreme and the intermediate parameter values are shown in Fig. 1 a–c. Examples of simulation results of $c_\mathrm{A}(t,z)$ and $\theta_\mathrm{A}(t,z)$ are shown in Figs. 2 and 3. The model (Eqs. (4), (5a), and (5b)) necessarily develops a gas phase concentration gradient inside the particle, as shown in Fig. 2. There is a gradient in the surface coverage as well, except in the (unrealistic) case of negligible readsorption. However, even minor readsorption immediately induces a gradient in the surface coverage.

Next we address the effect of readsorption in general. Fig. 4 a and b illustrate the significance of even very small readsorption ($k_\mathrm{a}(\mathrm{min})$ compared with (unrealistic) one-directional desorption ($k_\mathrm{a}(\mathrm{zero})$). Readsorption increases the retention time

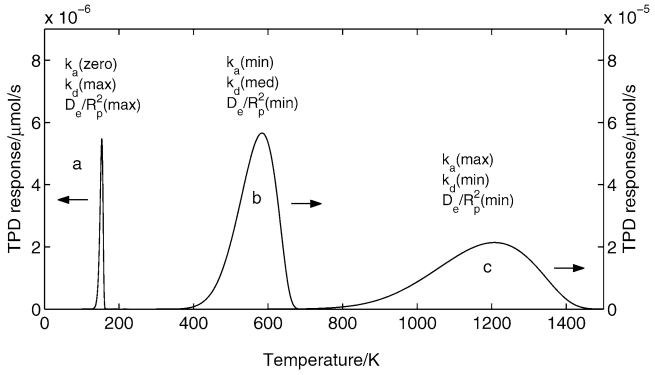

Fig. 1. Possible TPD responses in single particle simulations. TPD response in the lowest temperature range (a), an intermediate TPD response (b), and TPD response in the highest temperature range (c).

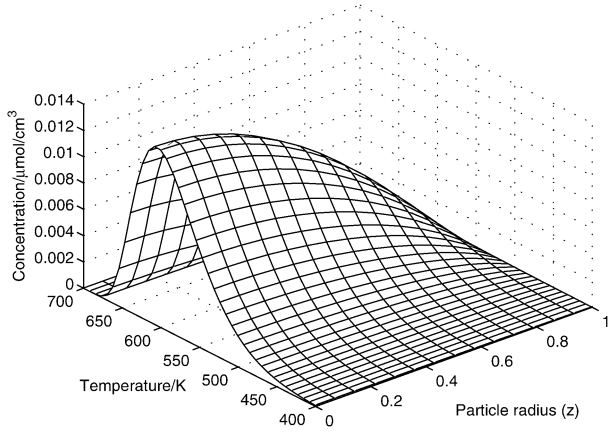

Fig. 2. Gas phase concentration, $c_A(T, z)$, in a single particle with k_a(min), k_d(med) and D_e/R^2 (min).

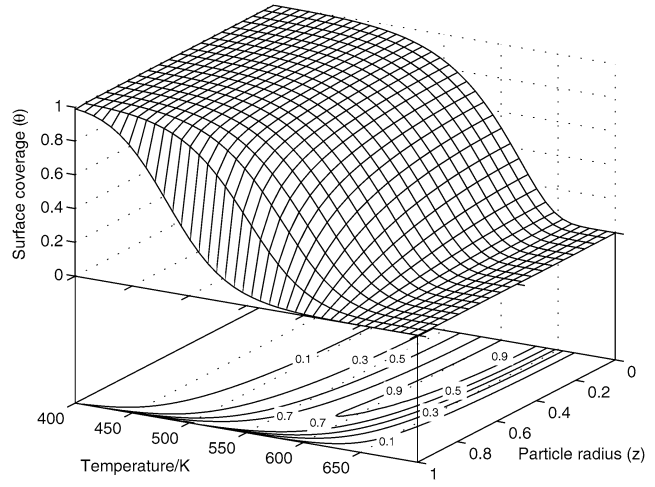

Fig. 3. (Top) surface coverage, $\theta_A(T, z)$, in a single particle with k_a(min), k_d(med) and D_e/R_p^2 (min). (Bottom) normalised contours of absolute derivatives of $\theta_A(T, z)$.

of the adsorbate in the particle and shifts the TPD response to higher temperatures. The simulations indicate that readsorption influences TPD responses over a very wide range of k_a. It seems that $k_a/(D_e/R_p^2)$ should be $<0.005\ \mathrm{cm}^3/\mu\mathrm{mol}$ to achieve essentially one-directional desorption.

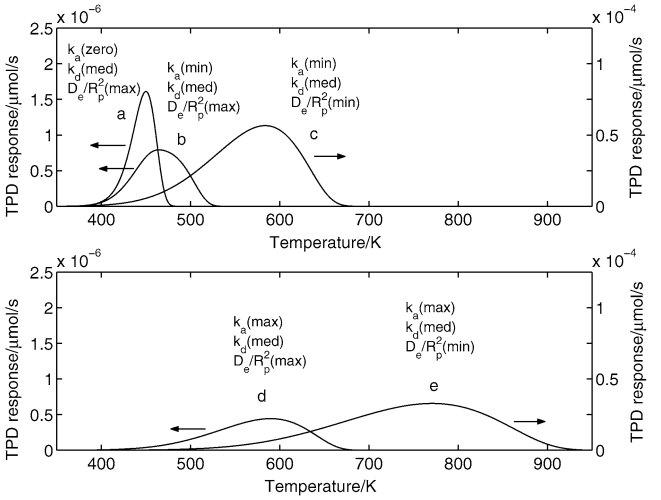

Fig. 4. TPD responses: without readsorption (a), minimum rate of adsorption (k_a(min)), medium rate of desorption (k_d(med)) and the two extreme values of D_e/R_p^2 (b and c), maximum rate of adsorption (k_a(max)), medium rate of desorption (k_d(med)) and the two extreme values of D_e/R_p^2 (d and e).

The specific effect of mass transfer rate in the presence of readsorption was studied by testing the effect of the rate of adsorption relative to the rate of diffusion (k_a(min/max) and D_e/R_p^2(min/max)) and by keeping the rate of desorption at the medium value (k_d(med)). The results, shown in Fig. 4, indicate that internal mass transfer rate (in a realistic range of TPD parameters) plays a role when readsorption is present. The stronger the readsorption, the more sensitive the output to the D_e/R_p^2 ratio. In the exceptional case of one-directional desorption, observable diffusion limitations occur only for $D_e/R_p^2 < 0.03\ 1/\mathrm{s}$, which is clearly outside the relevant parameter range (Table 3).

Next, we studied the occurrence of "quasi-equilibrium" between adsorption and desorption. Because the TPD experiment is transient, the local equilibrium between the gas phase and surface of the particle is called quasi-equilibrium. From the previous results, it seems apparent that readsorption always occurs to some extent if the rate of adsorption assumes values within the transition state theory. Some authors [9,11,13] have suggested that readsorption not only occurs in TPD, but also occurs to the extent needed to restore the adsorption–desorption equilibrium between the surface and the gas phase. In such a case, the observable TPD response is not in the kinetically controlled regime, but rather in the thermodynamically controlled regime.

To determine whether TPD of a single particle proceeds in quasi-equilibrium adsorption or deviates from it significantly, we first derive a single particle model that readily incorporates the quasi-equilibrium assumption, then compare the solution of this model to the solution of Eq. (4). In quasi-equilibrium, the coverage and the concentration are no longer independent of one another. This allows us to omit one of the variables. On the basis of equilibrium,

$$\theta_A = \frac{k_a c_A}{k_d + k_a c_A} = \frac{K c_A}{1 + K c_A}, \tag{7}$$

where K represents k_a/k_d, the equilibrium constant. The temperature dependence of K is of the form

$$K = A\exp\left(-\frac{\Delta H}{RT}\right). \tag{8}$$

Taking the total differential of Eq. (7), we get

$$\frac{\partial\theta_A}{\partial t} = \frac{\partial\theta_A}{\partial c_A}\frac{\partial c_A}{\partial t} + \frac{\partial\theta_A}{\partial K}\frac{\partial K}{\partial t}. \tag{9}$$

The two partial derivatives of the surface coverage can be readily expressed as

$$\frac{\partial\theta_A}{\partial c_A} = \frac{K}{(1+Kc_A)^2} \tag{10}$$

and

$$\frac{\partial\theta_A}{\partial K} = \frac{c_A}{(1+Kc_A)^2}. \tag{11}$$

The partial derivative of K can be expressed as

$$\frac{\partial K}{\partial t} = \frac{K\beta\Delta H}{R(T_0+\beta t)^2}. \tag{12}$$

Substituting the partial derivatives into the model equation (Eq. (9)) and solving for $\partial c_A/\partial t$, we obtain

$$\frac{\partial c_A}{\partial t} = \frac{\frac{D_e}{R_p^2\varepsilon_p}\left(\frac{\partial^2 c_A}{\partial z^2}+\frac{2}{z}\frac{\partial c_A}{\partial z}\right) - \frac{\rho_p N_A}{\varepsilon_p}\frac{\partial K}{\partial t}\frac{\partial\theta_A}{\partial K}}{1+\frac{\rho_p N_A}{\varepsilon_p}\frac{\partial\theta_A}{\partial c_A}}. \tag{13}$$

The whole TPD system is now described by a single equation (Eq. (13)), because surface coverage can be found by the solution of Eq. (13) and the equilibrium condition (Eq. (7)). To quantify the difference between the responses of the full model (Eq. (4)) and the quasi-equilibrium model (Eq. (13)), we calculate the SRMSE between the two models in the temperature range that covers 99.9% of the TPD response of the model with a wider temperature range.

All extreme (min/max) rate combinations ($2^3 = 8$ cases) were tested to evaluate the deviation from the quasi-equilibrium during TPD of the single particle. In six cases, the TPD responses of the models were effectively identical (SRMSE $<$ 0.001). The combination of k_a(min), D_e/R_p^2(max), and both k_d(min/max) gave a moderate deviation between the TPD responses of the two models (SRMSE 0.090 and 0.087). The case with the greatest deviation is shown in Fig. 5. The ratio of the rate of adsorption to the rate of diffusion (k_a to D_e/R_p^2 ratio) appears to be decisive, whereas the rate of desorption seems to be secondary. It is possible to find a criterion for maintaining the quasi-equilibrium adsorption–desorption conditions by seeking the minimum k_a to D_e/R_p^2 ratio to achieve a sufficient match (SRMSE $<$ 0.0450) between the full model (Eq. (4)) and the quasi-equilibrium model (Eq. (13)). The criterion for the quasi-equilibrium adsorption–desorption condition then becomes

$$\frac{k_a}{D_e/R_p^2} \geqslant 1.8\ \text{cm}^3/\mu\text{mol}. \tag{14}$$

The validity of this criterion does not mean that the equilibrium strictly prevails throughout the particle, but does indicate that

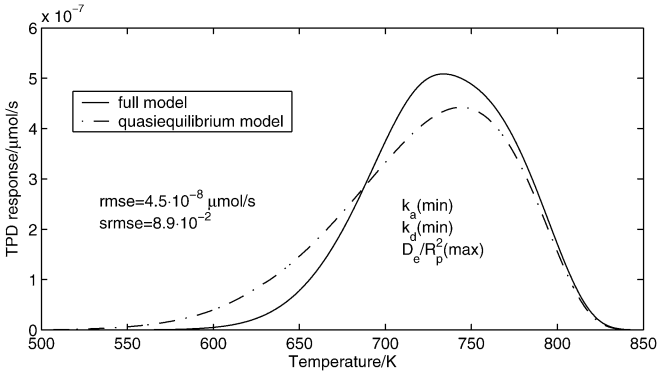

Fig. 5. The worst case in retaining the quasi-equilibrium in a single particle with infinite external mass transfer rate.

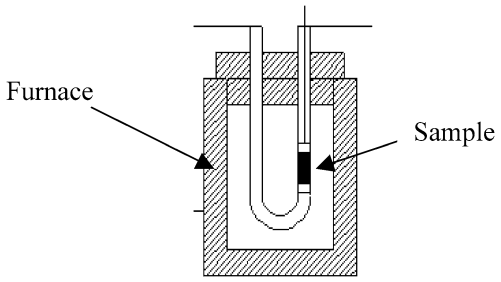

Fig. 6. Schematic presentation of a TPD reactor. Quartz u-tube placed in furnace.

the deviations are so minor or occur in such a limited volume at the outer boundary of the particle so that the overall flux from the particle is virtually unaffected.

The observations of Part I have significance for vacuum TPD setups and the entrance parts of flow TPD setups. The main findings are as follows:

1. Readsorption plays a significant role when the value of the adsorption constant is in the range suggested by the transition state theory.
2. When the readsorption is significant, the TPD response is sensitive to the rate of pore diffusion.
3. TPD in a single particle proceeds close to adsorption–desorption quasi-equilibrium over most of the studied parameter range.

3.2. Part II: Reactor model: description of a continuous-flow TPD reactor operating under atmospheric pressure

The typical ambient pressure TPD setup is a small-scale packed-bed reactor in which convection enters at one end and exits at the other (Fig. 6). Typically, in this TPD setup, the catalyst bed is shallow, and the particle-to-reactor diameter ratio is relatively high. Despite the evident packed-bed configuration, the kinetic analysis of TPD data is often preferentially carried out under the assumption of CSTR operation. The assumption of uniform concentration in the reactor simplifies the kinetic analysis and is especially required for the valid application of various Arrhenius plot-type analysis techniques. CSTR model requires either an efficient back-mixing or an otherwise uniform

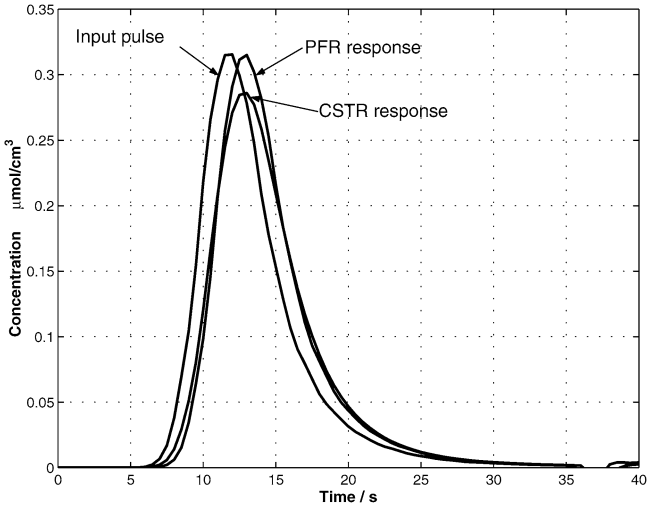

Fig. 7. Input pulse and simulated CSTR and PFR responses.

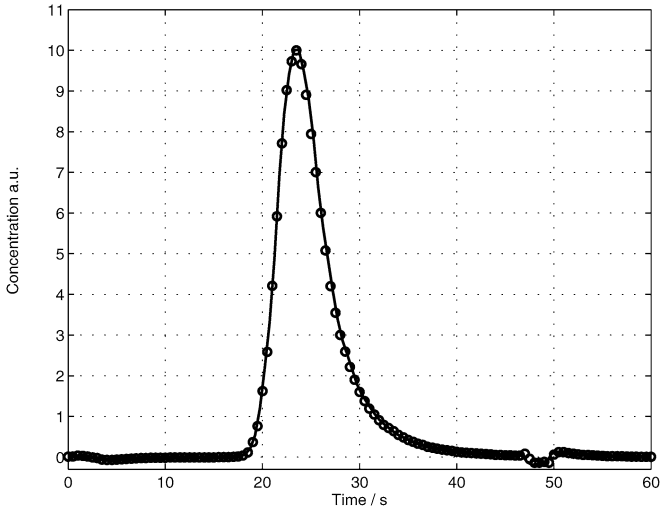

Fig. 8. Input pulse (—) and the pulse after travel through a reactor (○) packed with 1590 mg of crushed and sieved alumina ($d_p = 0.2$–0.4 mm). Both sets of data were obtained by averaging several measurements. Time shift has been applied to obtain superimposition to better allow comparison of pulses. The disturbances at the tail are due to switching of a valve.

axial profile of surface concentration (negligible readsorption). The plug flow reactor (PFR) model, although computationally a bit more demanding than the CSTR, is a possible choice for a reactor model, if it is physically valid. Serious challenges to kinetic analysis of TPD arise if the reactor cannot be adequately described as one of the ideal reactor models (CSTR or PFR). Technically, nonideal reactor models would not be too difficult to handle with present computational resources, but establishing the nonideal flow pattern and finding its parameters would make the kinetic analysis of TPD laborious. Thus, in what follows we consider conditions for selecting either CSTR or PFR as the reactor model for kinetic analysis of TPD.

In principle, the flow pattern of a TPD reactor can be experimentally tested by introducing tracer pulses that allow one to establish the flow residence time distribution. In practice, owing to the short space-time of the TPD reactor ($\ll$1 s), this would require special equipment to generate pulses with very rapid dynamics and a detection method with proportionate time resolution to distinguish even between the two extremes: the complete and negligible back-mixing (CSTR/PFR). Mechanisms for generating pulses in TPD apparatuses (e.g., for dosage of adsorbate or for calibration) are not suitable for investigating the flow pattern, because their dynamics are too slow (rise time $>$1 s) in relation to the space-time of the reactor and the sampling frequency (typically 2 1/s).

A simple test was carried out to probe the flow pattern of a TPD reactor. To circumvent the aforementioned problem, the space-time of the TPD reactor was increased up to $\sim$1.2 s by packing it with a massive amount (1590 mg) of inert porous material (alumina of particle size 0.2–0.4 mm). Pulses of hydrogen in argon were used as tracer signals. The dynamics of the input pulse were obtained by measuring the pulse through the empty reactor. If a considerable axial dispersion indicative of back-mixing is occurring in the system, then this experiment should reveal a broadening of the pulse after it passes though the packed bed. Fig. 7 shows the input pulse and the simulated PFR and CSTR responses to it at the outlet. Even now the difference between the extreme cases (CSTR and PFR) is not dramatic, but it is distinguishable. Although the broadening may be hard to see, any decrease in the peak height would be indicative of mixing in the flow pattern.

Fig. 8 illustrates an actual tracer experiment showing both the input pulse and the response measured after the packed bed. Both the illustrated input and response pulse were obtained by averaging several pulses to reduce the measurement noise. No pulse broadening or decrease in peak height was observed in these experiments. Because there was thus no sign of axial mixing, the flow pattern is considered to be suggestive of the plug flow in this TPD reactor.

Tracer studies, especially as depicted in Fig. 7, might lead one to think that the selection between CSTR and PFR models is unimportant because the pulse responses do not differ much, even for the extended packed bed. As Fig. 9 demonstrates, however, relatively minor readsorption introduces differences between the CSTR and PFR responses. Fig. 9 shows thermograms simulated using the CSTR and PFR model with a single combination of reaction parameters selected from the typical experimental parameter range. The observations regarding the two reactor responses were also essentially similar with other parameter combinations. It is evident that selection between the CSTR and PFR models in kinetic analysis is important, and the modelling attempts and the extraction of intrinsic kinetics might lead to very different results with the two reactor models.

Next, the mixing in the reactor and possible intermediate behaviour between the negligible and complete back-mixing (PFR/CSTR) were investigated. The tool here is the convection–axial dispersion reactor model (C-ADR), in which the axial dispersion term accounts not only for axial diffusion-type mixing, but also for radial mixing and other nonflat velocity profiles [22]. The three pseudohomogeneous reactor models are listed in Table 4. The extent of mixing in the C-ADR model is proportional to the reactor Peclet number, $\mathrm{Pe_r} = UL/D_a$, and its extreme values produce CSTR and PFR behaviours as asymptotic cases. When $\mathrm{Pe_r}$ goes to infinity, plug flow pattern

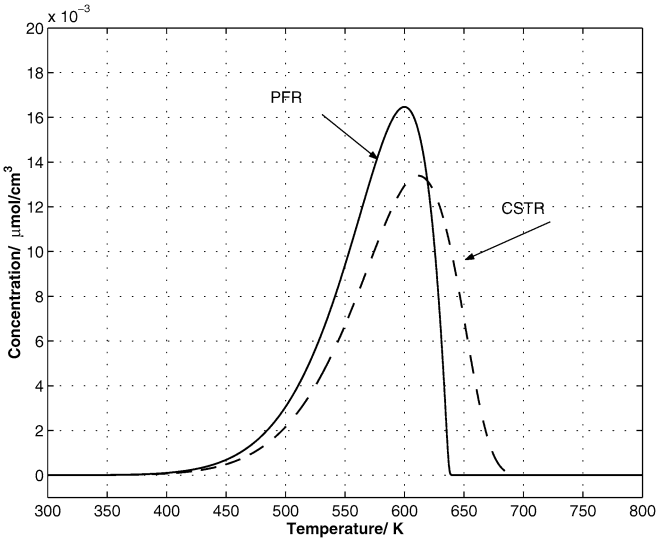

Fig. 9. TPD thermograms simulated using pseudohomogeneous PRF and CSTR models. Parameters: $m_{cat} = 30$ mg, $Q = 120$ ml/min, $L = 4$ mm, $d_b = 4$ mm, $k_a = 10^4$ cm^3/(µmol s), $k_d = 10^{13}\exp(-125kJ/(RT))$ 1/s. Other parameter values are the default values given in Table 2.

Table 4
Pseudohomogeneous reactor models

CSTR	$\frac{dc_A}{dt} = -\frac{1}{\tau(t)}c_A + \frac{(1-\varepsilon_b)\rho_p N_A}{\varepsilon_b}\left(-\frac{d\theta_A}{dt}\right)$
PFR	$\frac{dc_A}{dt} = -\frac{U(t)}{L\varepsilon_b}\frac{dc_A}{dx} + \frac{(1-\varepsilon_b)\rho_p N_A}{\varepsilon_b}\left(-\frac{d\theta_A}{dt}\right)$
C-ADR	$\frac{dc_A}{dt} = \frac{D_a}{L^2\varepsilon_b}\frac{d^2c_A}{dx^2} - \frac{U(t)}{L\varepsilon_b}\frac{dc_A}{dx} + \frac{(1-\varepsilon_b)\rho_p N_A}{\varepsilon_b}\left(-\frac{d\theta_A}{dt}\right)$

Table 5
Required reactor Peclet numbers (Pe_r) for ideal reactor behaviour

	$U_{min}L_{min}/D_a$	$U_{max}L_{max}/D_a$
CSTR	<0.7	<0.08
PFR	>2.7	>0.4

is approached. Correspondingly, Pe_r close to 0 introduces complete mixing.

The extreme cases in regard to mixing were studied with simulations of the C-ADR model in the range of typical TPD experimental parameters. These cases involved the extreme values of U and L with other simulation parameters kept constant because the flow pattern results are not sensitive to them. The axial dispersion coefficient D_a was adjusted until the desired ideal reactor behaviour (PFR or CSTR) was obtained. Table 5 lists the reactor Peclet numbers, Pe_r, required to achieve CSTR and PFR operation for extreme U and L values. The Peclet numbers reported were evaluated at 273.15 K for the empty tube, with Pe_r increasing during TPD. The responses of ideal reactors and C-ADR were considered equal for SRMSE < 0.0450. Table 5 gives limiting Pe_r values for interpretation of the TPD experiments. It is at least safe to assume CSTR if $Pe_r < 0.08$ and PFR if $Pe_r > 2.7$. For $0.08 < Pe_r < 2.7$, there is a transition region in which the reactor behaviour might be nonideal.

We now consider literature dealing with axial dispersion coefficients in packed beds. Data from Levenspiel [23] provides information on the inverse of the particle Peclet number ($1/Pe_f = D_a\varepsilon_b/(Ud_p)$) as a function of Reynolds number (Re). The required material properties of gases for Ar, He, and air were applied. The range of Re in the literature [23] does not cover all of the values occurring in TPD, but the range that is presented gives about $1/Pe_f = 0.5$. Sherwood et al. [24] covered a broader range of Re and provided $Pe_f \sim 2$. Butt [25] reported Pe_f as a function of Re multiplied by the Schmidt (Sc) number. Again, Pe_f is close to 2 for Re Sc values in TPD. Thus, the references reporting the magnitude of Pe_f are in agreement. Furthermore, the magnitudes of the axial dispersion coefficient, D_a result in $Pe_r = UL/D_a > 16$, which clearly fulfils the requirements for PFR operation.

From the foregoing theoretical considerations and the experimental test results, the plug flow reactor model was found to be preferable to describe the TPD reactor in the further studies. These conclusions apply to the packed-bed-type flow TPD setups in the typical range of experimental TPD parameters.

3.3. Part III: Heterogeneous model of TPD system: PFR + pore diffusion + intrinsic kinetics

In what follows we conduct simulations with a model describing the TPD system as a whole. The reactor is described by the plug flow reactor model based on the findings of Part II, and the particle dynamics are connected to the reactor mass balances through the diffusive flux from the particles. Intraparticle dynamics cover the intrinsic adsorption and desorption kinetics and the pore diffusion. The model is described by the particle and the reactor mass balances,

$$\frac{dc_A}{dt} = \frac{D_e}{R_p^2\varepsilon_p}\left(\frac{d^2c_A}{dz^2} + \frac{2}{z}\frac{dc_A}{dz}\right) + \frac{\rho_p N_A}{\varepsilon_p}\left(-\frac{d\theta_A}{dt}\right) \quad (15)$$

and

$$\frac{dc_A}{dt} = -\frac{U(t)}{L\varepsilon_b}\frac{dc_A}{dx} - \frac{3D_e(1-\varepsilon_b)}{R_p^2\varepsilon_b}\frac{dc_A}{dz}|_{z=1}. \quad (16)$$

Both position coordinates have been nondimensionalised. The intrinsic kinetics are described by Eq. (1). The solution of the system requires the initial conditions $c_A(x, z, t = 0)$ and $\theta_A(x, z, t = 0)$, two boundary conditions for Eq. (15), and a boundary condition for Eq. (16). In fact, Eq. (16) is one boundary condition for Eq. (15), the other being the symmetry condition at the particle core (Eq. (5a)). The boundary condition for Eq. (16) in TPD is

$$c_A(0, 1, t) = 0. \quad (17)$$

The study focuses on the system behaviour as a whole in the selected parameter range, with special focus on possible concentration gradients in the particle. Also of interest is the extent of readsorption as measured by the difference from the quasi-equilibrium between adsorption and desorption in the whole system. Again, the extreme behaviour is investigated by varying four groups of parameters essential to the system dynamics while keeping the less significant ones constant. The essential

Table 6
Parameters applied in the heterogeneous TPD model (Eqs. (15) and (16))

k_a (cm^3/(μmol s))	k_d (1/s)	$1/\tau$ (1/s)	D_e/R_p^2 (1/s)
$k_a(\min) = 10^4$	$k_d(\min) = 10^{13}\exp(-200kJ/(RT))$	$1/\tau\ (\min) = 0.27$	$D_e/R_p^2\ (\min) = 25$
$k_a(\max) = 10^7$	$k_d(\max) = 10^{16}\exp(-50kJ/(RT))$	$1/\tau\ (\max) = 99.5$	$D_e/R_p^2\ (\max) = 18750$

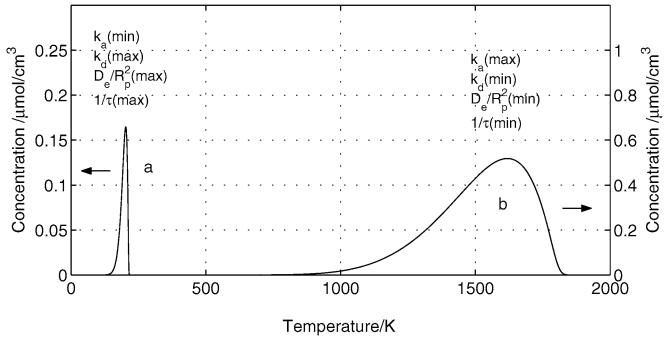

Fig. 10. The extreme TPD responses of the heterogeneous TPD model (Eqs. (15) and (16)).

parameters to vary in the simulations are the kinetic parameters of adsorption (k_a) and desorption (k_d), the D_e/R_p^2 ratio, and the inverse of the space-time of the reactor $1/\tau = U(t)/L\varepsilon_b$. Table 6 lists the range of values of the parameters. Because $1/\tau$ varies, it is reported at 273.15 K. The two extreme simulated TPD responses in the parameter range are presented in Fig. 10.

3.3.1. Intraparticle gradients in PFR

First, a convenient measure for "significant intraparticle gradients" is established. The simulated TPD response of the heterogeneous model at the reactor outlet is compared with that obtained with the pseudohomogeneous PFR model (Table 4). This immediately uncovers diffusion-limited occasions of practical importance. If the thermograms are equal (SRMSE < 0.0450), then the intraparticle gradients are insignificant and can be ignored.

Presumably, the degree of the intraparticle concentration gradients is governed mainly by the relation of the rates of external and internal mass transfer, whereas the intrinsic kinetics are expected to play a lesser role. In the previous single-particle simulations with infinite external mass transfer rate, concentration gradients were always present. The steepness of the gradients in the heterogeneous TPD model simulations is proportional to the ratio of $1/\tau$ ($\propto$ external mass transfer rate) to D_e/R_p^2 ($\propto$ internal mass transfer rate). Consequently, the steepest gradients should emerge in a simulation with the minimum reactor volume, the maximum flow rate, and the minimum D_e/R_p^2 ratio. Fig. 11 depicts this case with all four extreme kinetic parameter combinations and the SRMSE values between the two models, calculated in the 99.9% range of the heterogeneous model. As Fig. 11 clearly demonstrates, the heterogeneous TPD model and the pseudohomogeneous model give different results for all extreme combinations of the intrinsic kinetic parameters. Clearly, intraparticle diffusion limitations cause concentration gradients that are of practical significance. The greatest deviation (SRMSE) between the two models appears with $k_d(\min)$ and $k_a(\max)$. The combination of $1/\tau$ (max), D_e/R_p^2 (min), $k_d(\min)$, and $k_a(\max)$ is thus studied further to find the parameter range corresponding to diffusion-unlimited conditions. The key idea is to adjust the experimental

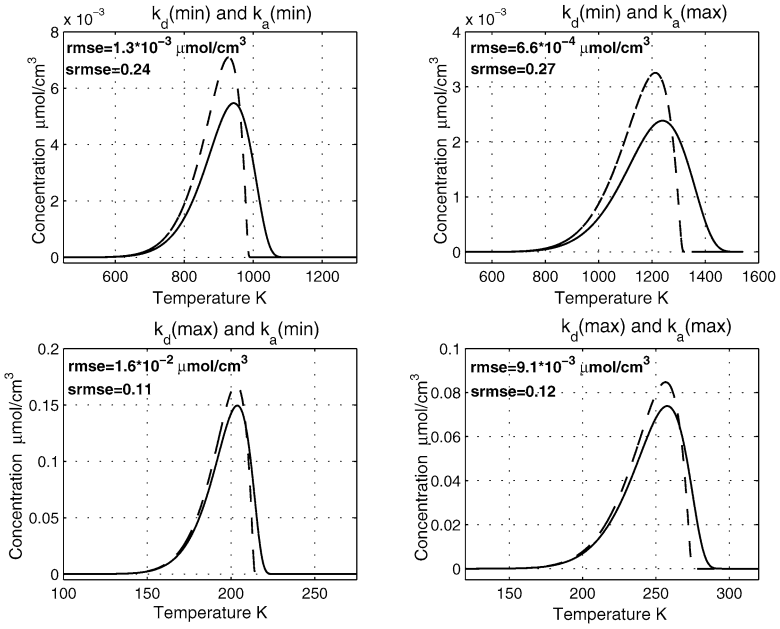

Fig. 11. Demonstration of the effect of the worst case intraparticle diffusion limitations to the TPD response obtained by simulating the heterogeneous TPD model (—) with $1/\tau$ (max) and D_e/R_p^2 (min) and four combination of intrinsic rates and the pseudohomogeneous model response (- - -).

details so that diffusion does not affect TPD responses. (The responses simulated by the pseudohomogeneous and the heterogeneous TPD model are approximately equal.)

Simulations were run with the worst-case parameter combination ($1/\tau$ (max), D_e/R_p^2 (min), k_d(min), and k_a(max)) and by relaxing one controllable experimental parameter (Q, m_{cat}, or R_p) at a time while keeping the rest constant, to evaluate the effect on the TPD responses. The main results can be summarised as follows:

1. The controllable experimental parameters (m_{cat}, Q, and R_p) can be adjusted to circumvent the diffusion limitations. The ratio of $1/\tau$ to D_e/R_p^2 needs to be decreased from the worst-case value (∼4) by a factor of 25 or more to achieve this.
2. One way to avoid intraparticle diffusion limitations is to increase the catalyst mass, decrease the flow rate, and, above all, grind the catalyst to a smaller particle size. Reducing the particle size to 0.004 cm is in itself a sufficient measure. The increase in m_{cat} (e.g., from 30 to 150 mg) should be accompanied by decrease of Q (e.g., from 120 to 20 cm^3/min) to achieve a practically diffusion unlimited case.
3. These observations are of significance for catalysts in which the intraparticle mass transfer occurs with the effective diffusion coefficient close to 0.01 cm^2/s (∼Knudsen diffusion, microporous materials).
4. For a general experimental parameter combination (Table 6), a criterion for negligible intraparticle diffusion limitations may be set up as

$$\frac{1/\tau}{D_e/R_p^2} = \frac{QR_p^2\rho_p(1-\varepsilon_b)}{D_e m_{cat}\varepsilon_b} < 0.16. \tag{18}$$

Findings 1–3 were based on the simulations of the worst case: $1/\tau$ (max), D_e/R_p^2 (min), k_d(min), and k_a(max). To ascertain that Eq. (18) is not too sensitive to the applied intrinsic kinetics, the three other extreme combinations of kinetic parameters were tested. The criterion (Eq. (18)) was found to be valid in the studied range (Table 6). When this criterion holds, the TPD reactor can safely be described as a pseudohomogeneous PFR.

3.3.2. Quasi-equilibrium adsorption in PFR

We next focus on possible quasi-equilibrium adsorption, that is, a situation in which local and temporal adsorption–desorption equilibrium prevails during the progress of TPD. The single-particle simulations (Section 3.1—Part I) investigated the interplay between the internal mass transfer rate and intrinsic kinetics and suggested that for most cases, the quasi-equilibrium adsorption/desorption is closely followed. Because Part I (Section 3.1) covers the situations of strong intraparticle gradients, we exclude the diffusion limitations here by assuming that the criterion of Eq. (18) now holds. Thus, the pseudohomogeneous model is applied in the simulations. The investigations focus on the deviations induced by the reactor dynamics, that is, competition between the external mass transfer rate and the intrinsic kinetics. The worst-case parameter combination with respect to maintaining the quasi-equilibrium is k_a(min) and $1/\tau$ (max). For this combination, we test the extreme desorption rates with k_d(min) and k_d(max).

A pseudohomogeneous PFR model incorporating the quasi-equilibrium assumption is derived. We eliminate θ_A on the basis of equilibrium in an analogous manner to Eqs. (7) and (8). Again using Eqs. (10) and (11), and substituting the partial derivatives to the pseudohomogeneous reactor model and solving for $\partial c_A/\partial t$, now provides

$$\frac{\partial c_A}{\partial t} = \frac{-\frac{U}{L\varepsilon_b}\frac{\partial c_A}{\partial x} - \frac{1-\varepsilon_b}{\varepsilon_b}\rho_p N_A \frac{\partial K}{\partial t}\frac{\partial \theta}{\partial K}}{1+\frac{1-\varepsilon_b}{\varepsilon_b}\rho_p N_A \frac{\partial \theta}{\partial c_A}}. \tag{19}$$

Note that the whole system is now described by one equation (Eq. (19)) for c_A, and θ_A can be found by the solution of Eq. (19) and the equilibrium condition Eq. (7).

The solution of the quasi-equilibrium model (Eq. (19)) and the previously obtained worst-case solution in regard to maintaining the quasi-equilibrium (the solution of the PFR model with k_a(min) and $1/\tau$ (max)) were compared for both k_d(min) and k_d(max). The match was outstanding. In the parameter range investigated, all of the thermograms were dominated by quasi-equilibrium adsorption/desorption.

The findings of the simulations with the heterogeneous TPD model can be summarised as follows:

1. There is a range of TPD parameters in which intraparticle concentration gradients are significant; however, intraparticle diffusion limitations may be avoided by adjusting the catalyst mass, particle size, and volumetric flow rate. A quantitative criterion (Eq. (18)) was set up for this purpose.
2. The quasi-equilibrium adsorption determines the dynamics of TPD in PFR. If the intraparticle diffusion limitations have been excluded, then the reactor may be described as pseudohomogeneous PFR with the quasi-equilibrium assumption incorporated.

4. Discussion

We discuss the kinetic analysis of experimental TPD data in the context of our simulation results and the literature on TPD methodology. The simulations carried out provided information about TPD in a defined range of system parameters, and the conclusions drawn hold in this domain and can reasonably be expected to be applicable in a wider range. For most parameters, the relevance of the considered parameter range (Table 2) can be validated against the reported literature. The effect of particular type of intrinsic kinetics is a more intricate matter. However, the conclusions presented are sensitive not to the exact form of the intrinsic kinetics, but rather (and more importantly) to the order of magnitude of the rates. Thus we consider that the first-order kinetics applied here, parameterised as reported, provide a sufficiently wide spectrum of rates and consequently sufficiently generality.

Table 7
Parameters suggested by Demmin and Gorte [14] translated into notation used in this work and evaluated in a typical TPD parameter range (Table 2)

Dimensionless parameter	Tested effect	Minimum value	Maximum value	Requirement according to D and G
D-G 1: $\frac{\varepsilon_b L \pi d_b^2 \beta}{4Q(T_f - T_0)}$	Convective lag	8.38×10^{-7}	7.85×10^{-3}	<0.01
D-G 2: $\frac{\varepsilon_b R_p^2 \beta}{D_e(T_f - T_0)}$	Diffusive lag	1.78×10^{-9}	3.33×10^{-5}	<0.01
D-G 3: $\frac{\rho_p R_p^2 Q}{3 m_{cat} D_e}$	Particle concentration gradients	3.12×10^{-6}	8.89×10^{-1}	<0.05
D-G 4: $\frac{4QL}{\pi d_b^2 D_a}$	Bed concentration gradients	3.40×10^{-1}	1.27×10^{2}	<0.1
D-G 5: $\frac{N_{tot} \rho_p R_p^2}{3 D_e} k_a$	Readsorption at infinite flow rate	3.56×10^{1}	1.60×10^{8}	<1
D-G 6: $\frac{N_{tot} \rho_p \pi d_b^2 L(1-\varepsilon_b)}{4Q} k_a$	Readsorption at low flow rate	3.02×10^{4}	1.13×10^{10}	<1

4.1. Criteria for TPD experiments and their interpretation

Gorte [11] and Demmin and Gorte [14] have presented design parameters for TPD from porous catalysts for cell-type (i.e., catalyst slab in CSTR) and packed-bed-type TPD setups. Their design parameters were obtained by nondimensionalising physical continuity equations equivalent to ours. The derived dimensionless parameters measure the readsorption effects, intraparticle gradients, gradients across the catalyst bed, lag times due to diffusion, and flow dynamics. Dimensionless parameters (denoted below as D-G parameters) are actually ratios of rates of elementary dynamic processes. The work of Demmin and Gorte [14] provides a convenient basis for our discussion.

Here we evaluate the minimum and maximum values of the dimensionless D-G parameters in the typical range of TPD parameters (Table 2) and compare them with the suggested ideal requirements, which we also assessed. We also examine the D-G parameters against our simulation results. Table 7 shows the D-G parameters [14] in our notation, and their minimum and maximum values are evaluated in the typical parameter range of TPD.

D-G 1 measures the ratio of space-time of the reactor to the total time of the experiment, and D-G 2 measures the corresponding ratio of the time constant of diffusion. The values of D-G 1 and D-G 2 suggest that these convective and diffusive lags are always negligible. This is usually taken care of in the design of the TPD equipment. Criteria D-G 1 and D-G 2 are therefore unnecessary if the parameters of the TPD are in the range defined in Table 2. Here the total temperature range, T_f–T_0, was assumed to be 200–1000 K.

D-G 3, the ratio of carrier gas flow rate to the rate of diffusion, indicates the existence of possible particle concentration gradients. If the ratio is <0.05, then intraparticle concentration gradients can be considered negligible. The values of D-G 3 indicate that intraparticle diffusion plays a role over a part of the parameter range. This criterion is analogous to our Eq. (18), differing only in constant $3(1-\varepsilon_b)/\varepsilon_b$. Equation (18) as translated into D-G 3 would be $0.16/4.5 = 0.036$, a bit stricter than D-G 3, but the order of magnitude would be the same.

Parameter D-G 4 is the reactor Peclet number, that is, the ratio of carrier gas flow rate to axial mixing. The value of D-G 4 depends on the axial dispersion coefficient, which is not usually readily available. Here the value of 0.5 cm^2/s for the axial dispersion coefficient is used to evaluate the minimum and maximum values of D-G 4. These values suggest that perfect mixing cannot be achieved by natural nonideal flow (back-mixing and turbulence). If perfect mixing were desirable, then a completely different TPD reactor construction should be considered. We also investigated the behaviour of the convection-axial dispersion model in a typical range of TPD parameters and established limits for the reactor Peclet number (Pe_r) to produce either CSTR or PFR behaviour. The extreme values of $U \cdot L$ were considered separately. D-G 4 agrees fairly well with our criterion for $Pe_r = U_{max} L_{max}/D_a$ for the CSTR operation. More importantly, PFR operation—and not CSTR or something between the CSTR and PFR—is predominant in the investigated parameter range. Demmin and Gorte [14] were concerned that achieving perfect mixing would not be realistic with flow rates of real TPD experiments, and that this would undermine attempts at kinetic analysis. However, dismissing CSTR as a reactor model for the TPD flow setup is not a problem. If the parameters of a TPD experiment fall into the range of the parameters of Table 2, then the PFR model can and should be used in kinetic analysis of TPD.

It has been claimed [13] that making the catalyst bed shallow would bring the reactor dynamics closer to CSTR behaviour and facilitate kinetic interpretation of the TPD thermograms. The assumption has been that a shallow packed bed operates in an essentially uniform concentration. The flow type in the typical TPD setup, as shown, is like plug flow in practice, which means that the entrance to the reactor is governed by a steep concentration gradient. The shallower the bed, the greater the part of the reactor exposed to this concentration gradient, and the reactor operation is far from CSTR. The part at the entrance is also always susceptible to intraparticle concentration gradients, and in this respect as well, a shallow reactor becomes ill-defined. Consequently, in a good reactor design, the bed length should exceed the reactor diameter. In this way, the entrance part constitutes a smaller fraction of the total bed length and the intraparticle concentration gradients at the entrance do not influence the total thermogram, and thus the pseudohomogeneous PFR may well be applied in kinetic interpretation of TPD

data. This of course also requires that the criterion described by Eq. (18) is satisfied.

Parameter D-G 5 measures the ratio of adsorption rate to diffusion rate. This parameter is viable for measuring the absence of readsorption when the external mass transfer rate is infinite. There is a minor error in the original criterion D-G 5 [14]: π^2 in the denominator should be 3. The values of D-G 5 indicate that D-G 5 <1 does not hold in the typical parameter range and that readsorption is always present. This is in line with our observations in the single-particle simulations. Simulations outside the parameter ranges (Table 2) show that D-G 5 as such is of the correct order of magnitude. However, the criterion D-G 5 cannot be met if the rate of adsorption assumes values within the transition state theory. Another conclusion from the single-particle simulations was that if the experimental setup involves a rapid external mass transfer rate, then the TPD response is dependent on both the adsorption and diffusion rates. Identifying intrinsic kinetics then requires that the diffusion rate be either known or studied simultaneously. Distinguishing intrinsic kinetics from mass transfer necessitates TPD experiments with different particle sizes, although with a uniform size per run. An uncontrolled particle size distribution in a diffusion-limited TPD case makes attempts at kinetic analysis pointless.

Parameter D-G 6 measures the ratio of adsorption rate to carrier gas flow rate. This parameter is suitable for measuring the absence of readsorption when TPD occurs in a flow reactor, and its values in the typical parameter range again indicate the definite presence of readsorption. Our simulations with the pseudohomogeneous PFR model confirmed that the theoretical rate of adsorption should be very low to produce a TPD response equal to one-directional desorption response; that is, the k_a to $(1/\tau)$ ratio should not exceed about 5×10^{-4} cm^3/μmol. This value is translated to D-G 6 by multiplying it by $N_{tot}\rho_p(1-\varepsilon_b)/\varepsilon_b$, giving ∼0.4. Thus again, the order of magnitude is about the same as that suggested by Demmin and Gorte [14]. In practice, readsorption not only plays a role in the plug flow reactor operation, but also even occurs to the extent of quasi-equilibrium adsorption/desorption in the typical parameter range. Experimental parameters cannot be adjusted within this typical range to give an adsorption-free situation, making the determination of pure desorption kinetics (ignoring adsorption) from thermograms impossible. Furthermore, in the quasi-equilibrium situation, the parameters of adsorption and desorption can be determined, but not uniquely, and only their ratio is meaningful. If the quasi-equilibrium between adsorption and desorption of a substance prevails under the conditions of TPD, then the adsorption/desorption of the substance during the operation of a real catalytic process proceeds in quasi-equilibrium at an even greater likelihood. Thus information on equilibrium might be more meaningful and valuable for practical purposes than information on desorption kinetics only. On the other hand, if a study of one-directional desorption kinetics is desired, then only UHV TPD in combination with nonporous material is applicable.

In summary, the D-G parameters as such have been found to be sound and the ideal requirements suggested in [14] are of the correct order of magnitude. In the typical range of TPD conditions and parameters, however, only D-G 3 is relevant. Accordingly, if the parameters of a TPD system lie in the ranges defined in Table 2, then only checking intraparticle diffusion limitations by either D-G 3 or our Eq. (18) is needed.

A phenomenological well-defined extrinsic description can be devised for TPD for high-surface area samples when the TPD setup involves continuous flow under ambient pressure. Kinetic analysis may be carried out according to general transient kinetic methodology, that is, nonlinear regression analysis involving model fitting to multiple complete experimental TPD patterns. Once proper extrinsic description is accomplished, experimental TPD data with rich information content are needed to test hypotheses on intrinsic kinetics and to estimate kinetic parameters. Kinetic models provide information on fundamental gas–solid interactions, and kinetic analysis of TPD is a potential tool for studying the microkinetics [20,26,27] of heterogeneous catalysis.

5. Conclusion

TPD is a convenient tool for catalyst characterisation, but its full utilisation calls for careful transient kinetic analysis, which should be based on a physicochemical description of the TPD system. This work focused on investigating the description of the extrinsic dynamics of TPD of porous catalysts in an atmospheric flow setup. First, a typical range of TPD parameters was defined. The simulation work was divided into three parts. Simulations of a single catalyst particle with infinite external mass transfer rate (Section 3.1—Part I) revealed that readsorption played a role with all realistic values of material and kinetic parameters and that the simulated TPD patterns were very sensitive to the intraparticle mass transfer rate. Separate investigations on the reactor flow model (Section 3.2—Part II) for a continuous-flow packed-bed TPD setup under atmospheric pressure clearly advocated the application of the PFR model instead of the CSTR model. Finally, based on the results of Parts I and II, a complete heterogeneous TPD simulation model (PFR + intraparticle diffusion + intrinsic kinetics) was established (Section 3.3—Part III). The results of Part III confirmed that it is possible to adjust experimental conditions and properties to collect experimental TPD data undisguised by intraparticle diffusion limitations, and that under those conditions, the pseudohomogeneous PFR model may be applied in kinetic analysis. Furthermore, the readsorption during TPD must be accounted for in the model, likely up to the adsorption/desorption quasi-equilibrium. If the quasi-equilibrium prevails during TPD, then kinetic analysis provides adsorption equilibrium information instead of strictly kinetic information.

The main conclusion of this work is that a phenomenological well-defined extrinsic description can be devised for TPD of porous catalysts in setups involving continuous flow under ambient pressure. A valid description of extrinsic dynamics is a prerequisite for a sound transient kinetic analysis.

Appendix. Symbol list

A	pre-exponential factor
c_A	gas phase concentration of desorbing component A
d_b	bed diameter (cm)
D_a	axial dispersion coefficient (cm^2/s)
D_e	effective diffusivity in particle (cm^2/s)
ΔH	adsorption enthalpy (kJ/mol)
k_a	rate constant of adsorption ($cm^3/(\mu mol\,s)$)
k_d	rate constant of desorption (1/s)
K	adsorption equilibrium constant ($cm^3/\mu mol$)
L	bed length (cm)
m_{cat}	catalyst weight (mg)
N_A	number of adsorption sites on the catalyst ($\mu mol/mg_{cat}$)
Pe_f	particle Peclet number
Pe_r	reactor Peclet number
Q	flow rate of carrier gas in empty tube (cm^3/min)
R	universal gas constant
R_p	radius of particle (cm)
t	time (s)
T	temperature (K)
T_0	initial temperature in TPD (K)
T_f	final temperature in TPD (K)
U	superficial velocity (cm/s)
W	flux (through outer surface of particle)
x	dimensionless axial coordinate of reactor
z	dimensionless radial coordinate of spherical particle

Greek symbols

β	heating rate (K/min)
ε_b	bed porosity
ε_p	particle porosity
θ_A	surface coverage of desorbing component A
ρ_p	catalyst density (mg/cm^3)
τ	space-time of packed bed reactor (s)

Supplementary material

The online version of this article contains additional supplementary material.

Please visit doi:10.1016/j.jcat.2005.12.026.

References

[1] P.A. Redhead, Vacuum 12 (1962) 203.
[2] R.J. Cvetanovic, Y. Amenomiya, Adv. Catal. 17 (1967) 103; [1].
[3] J.W. Niemantsverdriet, Spectroscopy in Catalysis an Introduction, second ed., Wiley–VCH, Weinheim, 2000.
[4] R.J. Gorte, Catal. Today 28 (1996) 405.
[5] J.L. Falconer, R.J. Madix, J. Catal. 48 (1977) 262.
[6] J.A. Konvalinka, J.J.F. Scholten, J.C. Rasser, J. Catal. 76 (1977) 365.
[7] E.E. Ibok, D.F. Ollis, J. Catal. 66 (1980) 391.
[8] J.A. Konvalinka, H. van Oeffelt, J.J.F. Scholten, Appl. Catal. 1 (1981) 141.
[9] R.K. Herz, J.B. Kiela, S.P. Marin, J. Catal. 73 (1982) 66.
[10] P.I. Lee, J.A. Schwarz, J. Catal. 73 (1982) 272.
[11] R.J. Gorte, J. Catal. 75 (1982) 164.
[12] J.L. Falconer, J.A. Schwarz, Catal. Rev.-Sci. Eng. 25 (1983) 141.
[13] J.S. Rieck, A.T. Bell, J. Catal. 85 (1984) 143.
[14] R.A. Demmin, R.J. Gorte, J. Catal. 90 (1984) 32.
[15] E. Tronconi, P. Forzatti, J. Catal. 93 (1985) 197.
[16] E. Tronconi, P. Forzatti, Chem. Eng. Sci. 41 (1986) 2541.
[17] P.-I. Lee, Y.-J. Huang, J.C. Heydweiller, J.A. Schwarz, Chem. Eng. Commun. 63 (1988) 205.
[18] Y.-J. Huang, J. Xue, J.A. Schwarz, J. Catal. 109 (1988) 396.
[19] T. Ioannides, X.E. Verykios, J. Catal. 120 (1989) 157.
[20] J.A. Dumesic, D.F. Rudd, L.M. Aparicio, J.E. Rekoske, A.A. Treviño, The Microkinetics of Heterogeneous Catalysis, ACS Professional Reference Book, Washington, DC, 1993.
[21] H.S. Fogler, Elements of Chemical Reaction Engineering, third ed., Prentice–Hall, Englewood Cliff, NJ, 1999, p. 741.
[22] H.S. Fogler, Elements of Chemical Reaction Engineering, third ed., Prentice–Hall, Englewood Cliff, NJ, 1999, p. 877.
[23] O. Levenspiel, Chemical Reaction Engineering, second ed., Wiley, New York, 1972.
[24] T.K. Sherwood, P.L. Pigford, C.R. Wilke, Mass Transfer, McGraw–Hill, Tokyo, 1975.
[25] J.B. Butt, Reaction Kinetics and Reactor Design, third ed., Prentice–Hall, Englewood Cliff, NJ, 1980.
[26] P. Stoltze, Prog. Surf. Sci. 65 (2000) 65.
[27] O. Hinrichsen, F. Rosowski, M. Mühler, G. Ertl, Stud. Surf. Sci. Catal. 109 (1997) 389.